International Journal of Financial Engineering
Vol. 4, No. 1 (2017) 1750014 (28 pages)

DOI: 10.1142/S2424786317500141

Pricing derivatives with fractional volatility

Hideharu Funahashi

Mizuho Securities Co. Ltd., Otemachi First Square 1-5-1, Otemachi Chiyoda-ku, Tokyo 100-0004, Japan

Received: 6 June 2016; Accepted: 6 February 2017
Published: 27 March 2017

Abstract

This paper studies the effect of fractional volatility on path-dependent options, which are highly sensitive to the volatility structure of a targeted underlying asset process. To this end, we propose an approximation formula for average and barrier options when volatility follows a fractional Brownian motion. Furthermore, using the analytical formula, we investigate the impact of the Hurst index on option prices. Overall, our important finding is that when the maturity is short and speed of mean-reversion is slow, the impact of the Hurst index strongly influences the option prices and that is non-negligible. This is an important lesson for practitioners who uses standard Brownian motion.

Keywords: Asian option; fractional Brownian motion; stochastic volatility model; mean-reverting process; hurst index; volatility persistence.

1. Introduction

The payoff of path-dependent options depends not only on the final values, but also on the sample paths of the prices of the underlying assets. For example, an average option, usually called an Asian option, is a path-dependent option whose payoff functions are determined by the average of underlying prices. They are less expensive than the corresponding vanilla options and provide corporate firms with ways to hedge risks arising from their business. Hence, they are popular in the equity, FX, and commodities market. Similarly, a barrier option is considered a path dependent option because its payoff depends on whether or not the underlying asset has reached a predetermined price. The option is called a knock-out type if

Email address: hideharu.funahashi@mizuho-sc.com

the right to exercise ceases to exist when the barrier is crossed, while it is called a knock-in type if the holder receives a new option upon hitting. The option is also classified as an up- or down-option, depending on the position relative to the spot prices at the start of the option. Barrier options are very popular in exchanges worldwide, as well as on the OTC market.

The path-dependability feature of the options makes them highly sensitive to the volatility structure of a targeted underlying asset process; thus, it is very important to model the volatility process appropriately. Numerous studies have attempted to characterize a good volatility model by its ability to capture commonly stylized facts about market-observed volatilities. Engle and Andrew (2001) outlined stylized facts about volatility that should be incorporated into a model. One important feature of the volatility process comes from the clustering of large and small fluctuations of asset prices. It is known that a large fraction of the asset price often induces other large fractions, and a small fraction induces other small fractions; this means that volatility shocks today will influence the expectation of volatility over many periods in the future.

Recently, there is a general consensus to consider that volatility displays some long memory. Several models have been proposed to capture this long-range memory feature including Bollerslev (1986), Nelson (1991), and Bollerslev and Mikkelsen (1996). Fractional Brownian motion is considered a prime candidate because of its tractability and similarity to the ordinary Brownian motion.

Fractional Brownian motion has been widely used in various scientific fields such as hydrology, communication technology, theoretical physics, statistics, biology and many others. As a result, many researchers have tackled the problem and developed various techniques that have been used to study this process. Nevertheless, fractional Brownian motion is still known to be difficult to treat both analytically and numerically since it is not a semi-martingale (expect in the Brownian motion case).

Motivated by empirical studies, fractional Brownian motion has also been steadily gaining attention in the field of finance. A fractional Black–Scholes model has been proposed as an improvement of the classical Black–Scholes model to express market behavior. Unfortunately, however, as Sottinen (2001), Rogers (1997), and Cheridito (2003) detected, fractional Black–Scholes model allows for arbitrage opportunities. By contrast, Hu and Øksendal (2003) developed a no-arbitrage model by introducing Wick integrals but this model cannot add a natural economic interpretation. Cheridito (2003) and Guasoni (2006) proved that arbitrage opportunity disappear when considering transaction costs and a minimal amount of time between transactions.

In the case of European options, it appears that the ordinal stochastic volatility model driven by traditional Brownian motion implies faster time-decay of the volatility smile when time to maturities increase faster than what we observe in the real market. Comte and Renault (1998) introduce a fractional volatility process in the Hull and White (1987) setting:

$$\begin{cases} \dfrac{\mathrm{d}S_t}{S_t} = \mu_t \mathrm{d}t + \sigma_t \mathrm{d}W_t, \\ \mathrm{d}(\log \sigma_t) = \kappa(\theta - \log \sigma_t)\mathrm{d}t + \gamma \mathrm{d}W_t^H, \end{cases} \tag{1.1}$$

where W_t^H is an fBM with Hurst index H, $0 < H < 1$. It is known that, if $H > 0.5$, the fBM is not Markovian and exhibits the long memory feature. On the other hand, if $H = 0.5$, the fBM is reduced to the standard Brownian motion, which is a Markov process with a short memory. They found that thanks to the long-memory feature of the volatility process, the decrease of the volatility smile amplitude with respect to time to maturity is slower than the traditional stochastic volatility models such as those of Hull and White (1987), Heston (1993), and Schöbel and Zhu (1999). This is a preferable feature since it is well-known that the observed smile amplitude does not decrease sufficiently fast with time to maturity to be explained by a short memory stochastic volatility. Xiao *et al.* (2010) considered currency options under an fBM with jumps.

Gatheral *et al.* (2014) found evidence of rough volatility by estimating volatility from high frequency data and showed that log-volatility behaves as a fBM with Hurst index H of order 0.1 at any reasonable time scale. Moreover, their model can capture the extra steepness of the implied volatility skew in Equity markets for short maturities. When H is close to zero, Alòs *et al.* (2007) and Fukasawa (2011) proved theoretically that the term structure of the at-the-money volatility skew can be approximated by a power-law function of time to maturity. Although these models cannot capture the long memory property of volatility, which is regarded as a stylized fact, there has been an increasing interests in rough volatility models.

Funahashi and Kijima (2017a) derived an accurate approximation formula for European contingent claims under general classes of fractional volatility models and provided numerical results to demonstrate how slowly the smile amplitude decreases. They show that the Hurst index under fractional volatility has a crucial impact on option prices especially when the maturity is short and the speed of mean-reverting is slow. However, note that the value of European options depends on the price of the underlying asset only at maturity point in time. On the other hand, the terminal value of Asian and barrier options depends upon the value of the underlying asset, not only at maturity, but also at prior points in time. In other words, the option's terminal value depends on the path take by the underling asset over the life time of the option. Hence, it can be expected that the volatility persistence (long-range dependence of the volatility process) more strongly influence Asian and barrier option prices than European option prices.

The aim of this paper is to develop an analytical approximation for the pricing of Asian and barrier options under fractional volatility models. In addition, utilizing this analytical formula, we investigate the impact of Hurst index on option prices. For this purpose, we extend an approximation formula proposed by Funahashi and Kijima (2017a) to average option and enlarge the approximation method proposed by Funahashi and Higuchi (2017) to barrier option. These methods are general enough to be applicable to the widely used option pricing models such as local volatility models, stochastic volatility models, and their combinations under fractional Brownian dynamics. The resulting approximation formula requires, at most, three-dimensional numerical integration; hence it can be computed quickly and is suitable for practical purposes. Furthermore, numerical tests demonstrate that the accuracy of our approximation is high enough for practical uses.

This paper is organized as follows. The next section describes the fractional volatility model. Then, approximation formulas for Asian and barrier option prices are derived in Sec. 3. Section 4 is devoted to numerical experiences to investigate the impact of the Hurst index on the option prices. Finally, Sec. 5 includes concluding remarks about this study.

Throughout this paper, the current time is fixed to be $t = 0$ and the option maturity is given by $T > 0$. Also, $(\Omega, \mathcal{F}, \mathbb{Q}, \{\mathcal{F}_t\}_{0\le t\le T})$ denotes a filtered probability space where the filtration $\{\mathcal{F}_t\}_{0\le t\le T}$ satisfies the usual conditions. The probability measure $\mathbb{Q}$ denotes a risk neutral measure. The expectation operator under $\mathbb{Q}$ is denoted by $\mathbb{E}$.

2. Setup

This paper assumes that the underlying asset price $\{S_t\}_{0\le t\le T}$ and its volatility $\{\sigma_t\}_{0\le t\le T}$ follow a stochastic differential equation (SDE):

$$\begin{cases} \dfrac{\mathrm{d}S_t}{S_t} = r\mathrm{d}t + f(\sigma_t)\mathrm{d}W_t, \\ \mathrm{d}\sigma_t = (\theta - \kappa\sigma_t)\mathrm{d}t + \epsilon \mathrm{d}W_t^H \end{cases} \tag{2.1}$$

under $\mathbb{Q}$, where r is risk free rate, f is an arbitrary smooth function of its argument, and $\{W_t\}_{t\ge 0}$ and $\{W_t^H\}_{t\ge 0}$ are a standard Brownian motion and fractional Brownian motion with Hurst index H, respectively. The volatility σ_t is a mean-reverting process. θ represents the long-term average of the volatility, ϵ denotes the volatility of volatility, and κ is the speed of mean reversion.

By adopting the formulation used by Comte and Renault (1998)[1], the fractional Brownian motion can be represented in term of stochastic integral with respect to another standard Brownian motion:

$$W_t^H = \int_0^t \lambda_1(t,s)\mathrm{d}\bar{W}_s, \tag{2.2}$$

where $0 \leq H \leq 1$, $\mathrm{d}\bar{W}$ is a standard Brownian motion with $\rho \mathrm{d}t = \mathrm{d}W_t \mathrm{d}\bar{W}_t$, and

$$\lambda_1(t,s) = \frac{1}{\Gamma(H+\frac{1}{2})}(t-s)^{H-\frac{1}{2}},$$

with the gamma function $\Gamma(a) = \int_0^\infty t^{a-1}\mathrm{e}^{-t}\mathrm{d}t$. This fractional integral is known as the Holmgren–Riemann–Liouville fractional integral coined by Lévy in 1953. For a detailed discussion, see Mandelbort and Ness (1968).

The SDE (2.1) is integrated as

$$\begin{cases} S_t = F(0,t)\exp\left(\int_0^t f(\sigma_s)\mathrm{d}W_s - \frac{1}{2}\int_0^t f^2(\sigma_s)\mathrm{d}s\right), \\ \sigma_t = V(0,t) + \int_0^t \lambda_2(t,s)\mathrm{d}\bar{W}_s, \end{cases} \tag{2.3}$$

where

$$\lambda_2(t,s) = \epsilon\left(\lambda_1(t,s) - \frac{\kappa^{\frac{1}{2}-H}\bar{E}(t)E(s)}{\Gamma(H+\frac{1}{2})}\int_0^{(t-s)\kappa} x^{H-\frac{1}{2}}\mathrm{e}^x \mathrm{d}x\right)$$

with $E(t) = \mathrm{e}^{\kappa t}$, $\bar{E}(t) = 1/E(t)$ and $V(0,t) = \sigma_0\bar{E}(t) + \theta(1-\bar{E}(t))$.

Like Funahashi and Kijima (2017a), this study assumes that the asset price S_t is approximated by the following 3rd-order chaos expansion:

Lemma 2.1. *Let $F(0,t) = S_0\mathrm{e}^{\int_0^t r(u)\mathrm{d}u}$ be the forward price of the underlying asset with delivery date t. Then,*

$$S_t \approx F(0,t)(1 + a_1(t) + a_2(t) + a_3(t)), \tag{2.4}$$

where

$$a_1(t) = \int_0^t \gamma(s)\mathrm{d}W_s,$$

[1]Instead of truncating the integral representation, we can consider the *true* fBM

$$W_t^H = \int_0^t \lambda_1(t,s)\mathrm{d}\bar{w}_s + \int_{-\infty}^0 ((t-s)^{H-\frac{1}{2}} - (-s)^{H-\frac{1}{2}})\mathrm{d}\bar{W}_s.$$

$$
\begin{aligned}
a_2(t) = &\int_0^t f_0(s)\left(\int_0^s f_0(u)\mathrm{d}W_u\right)\mathrm{d}W_s + \int_0^t f_0^{(1)}(s)\left(\int_0^s \lambda_2(s,u)\mathrm{d}\bar{W}_u\right)\mathrm{d}W_s,\\
a_3(t) = &\int_0^t f_0(s)\left(\int_0^s f_0(u)\left(\int_0^u f_0(r)\mathrm{d}W_r\right)\mathrm{d}W_u\right)\mathrm{d}W_s\\
&+\int_0^t f_0(s)\left(\int_0^s f_0^{(1)}(u)\left(\int_0^u \lambda_2(u,r)\mathrm{d}\bar{W}_r\right)\mathrm{d}W_u\right)\mathrm{d}W_s\\
&+\int_0^t f_0^{(1)}(s)\left(\int_0^s f_0(u)\left(\int_0^u \lambda_2(s,r)\mathrm{d}\bar{W}_r\right)\mathrm{d}W_u\right)\mathrm{d}W_s\\
&+\int_0^t f_0^{(1)}(s)\left(\int_0^s \lambda_2(s,u)\left(\int_0^u f_0(r)\mathrm{d}W_r\right)\mathrm{d}\bar{W}_u\right)\mathrm{d}W_s\\
&+\int_0^t f_0^{(2)}(s)\left(\int_0^s \lambda_2(s,u)\left(\int_0^u \lambda_2(s,r)\mathrm{d}\bar{W}_r\right)\mathrm{d}\bar{W}_u\right)\mathrm{d}W_s,
\end{aligned}
$$

where $f_0(t) = f(V(0,t))$, $f_0^{(n)}(t) = \partial_x^{(n)} f(x)|_{x=V(0,t)}$, *and*

$$\gamma(s) = f_0(s) + \rho f_0^{(1)}(s)\int_0^s f_0(u)\lambda_2(s,u)\mathrm{d}u + \frac{1}{2}f_0^{(2)}(s)\int_0^s \lambda_2^2(s,u)\mathrm{d}u.$$

3. Main Results

Before proceeding, let us consider the Asian and barrier options examined in this paper.[2]

For the time-t price, S_t, of a risky asset, its average is defined by

$$A_T = \frac{1}{T}\int_0^T S_s\mathrm{d}s. \tag{3.1}$$

Then, we consider a call option written on A_T with exercise price K, i.e.,

$$C^A(K,T) = \mathbb{E}[\mathrm{e}^{-\int_0^T r(u)\mathrm{d}u}(A_T - K)^+]. \tag{3.2}$$

Next, we formulate an up-and-in single barrier B with $S_0 < B$.[3] Let us denote the first hitting time of S_t to the barrier and the running maximum, respectively, by

$$\tau := \inf\{t \geq 0 : S_t \leq B\}, \quad S_0 < B, \tag{3.3}$$

[2]Our method can be used for more complex Asian options including fixed-strike, floating-strike, continuously sampled, discretely sampled, forward-start, and in-progress transactions. See Funahashi and Kijima (2017b) for details.

[3]This paper consider only the case of up-and-in barrier. The up-and-out, up-and-in, down-and-in, and down-and-out barrier cases can be treated similarly and hence omitted.

where $\tau = \infty$ if the event is empty, and

$$M_t^S := \max_{0 \le s \le t} S_s.$$

Then, the payoff of an up-and-in call option written on S_t with strike K and maturity T is given as

$$C^B(T,K) = \mathrm{e}^{-\int_0^T r(s)\mathrm{d}s} \mathbb{E}[g(S_T)], \tag{3.4}$$

where $g(X) = (X-K)^+ \chi_{M^X > B}$ and χ denotes the indicator function, i.e., $\chi_A = 1$ if A is true and $\chi_A = 0$ otherwise.

3.1. Asian option pricing formula

In Lemma 2.1, we have approximated the asset price S_t by a truncated sum of iterated Itô stochastic integrals. Using this result, the target random variable A_t can be approximated by integrating the both sides of (2.4) and changing integration order. The derivation is straightforward and, hence, omitted.

Corollary 3.1. *Let* $\bar{p}(T,s) := \frac{1}{T} p(s) \int_s^T F(0,u)\mathrm{d}u$. *Then,*

$$A_T \approx \bar{a}_0(T) + \bar{a}_1(T) + \bar{a}_2(T) + \bar{a}_3(T),$$

where

$$\bar{a}_0(T) = \frac{1}{T}\int_0^T F(0,s)\mathrm{d}s,$$

$$\bar{a}_1(T) = \int_0^T \bar{\gamma}(T,s)\mathrm{d}W_s,$$

$$\bar{a}_2(T) = \int_0^T \bar{f}_0(T,s)\left(\int_0^s f_0(u)\mathrm{d}W_u\right)\mathrm{d}W_s + \int_0^T \bar{f}_0^{(1)}(T,s)\left(\int_0^s \lambda_2(s,u)\mathrm{d}\bar{W}_u\right)\mathrm{d}W_s,$$

$$\begin{aligned}
\bar{a}_3(T) = &\int_0^T \bar{f}_0(T,s)\left(\int_0^s f_0(u)\left(\int_0^u f_0(r)\mathrm{d}W_r\right)\mathrm{d}W_u\right)\mathrm{d}W_s \\
&+ \int_0^T \bar{f}_0(T,s)\left(\int_0^s f_0^{(1)}(u)\left(\int_0^u \lambda_2(u,r)\mathrm{d}\bar{W}_r\right)\mathrm{d}W_u\right)\mathrm{d}W_s \\
&+ \int_0^T \bar{f}_0^{(1)}(T,s)\left(\int_0^s f_0(u)\left(\int_0^u \lambda_2(s,r)\mathrm{d}\bar{W}_r\right)\mathrm{d}W_u\right)\mathrm{d}W_s \\
&+ \int_0^T \bar{f}_0^{(1)}(T,s)\left(\int_0^s \lambda_2(s,u)\left(\int_0^u f_0(r)\mathrm{d}W_r\right)\mathrm{d}\bar{W}_u\right)\mathrm{d}W_s \\
&+ \int_0^T \bar{f}_0^{(2)}(T,s)\left(\int_0^s \lambda_2(s,u)\left(\int_0^u \lambda_2(s,r)\mathrm{d}\bar{W}_r\right)\mathrm{d}\bar{W}_u\right)\mathrm{d}W_s.
\end{aligned}$$

An important observation to note at this point is that average price, A_t, has the same structure as S_t in Lemma 2.1. In summary, the random variable $\bar{a}_1(T)$ follows a Wiener integral which follows a normal distribution with zero mean and variance

$$\bar{\Sigma}_T = \int_0^T \bar{\gamma}^2(T,s)\mathrm{d}s.$$

The random variable $\bar{a}_2(T)$ and $\bar{a}_3(T)$ are the second- and third-order iterated stochastic integral with deterministic integrands, respectively.

Note that, let $X_T := A_T - \bar{a}_0(T)$ and $\bar{K} = \bar{a}_0(T) - K$, the option price (3.2) is reduce to

$$C^A(K,T) = \mathrm{e}^{-rT}\int_{-\bar{K}_T}^{\infty}(x+\bar{K})f_{X_T}(x)\mathrm{d}x,$$

where f_{X_T} denotes the density function of X_T. Hence, to price the Asian option, it suffices to derive f_{X_T}.

In Appendix A, we derive the density function f_{X_T}. We remark that the approximated density function of A_t, denoted by $\tilde{f}_{A_t}(x)$, is also applicable as

$$f_{A_t}(x) = f_{X_t}(x - \bar{a}_0(t)). \tag{3.5}$$

Hence, calculating the integral in (3.2), we obtain the following result.

Theorem 3.1. *The value of an Asian call option with maturity T and strike K is approximated as*

$$\begin{aligned} C^A(T) \approx e^{-rT}\Bigg\{ & \frac{n(\bar{K};0,\bar{\Sigma}_T)}{2\bar{\Sigma}_T^4}[q_3(T)(\bar{K}^4 - 6\bar{K}^2\bar{\Sigma}_T + 3\bar{\Sigma}_T^2) \\ & + \bar{\Sigma}_T^2(q_4(T) + 2q_2(T))(\bar{K}^2 - \bar{\Sigma}_T) \\ & + \bar{\Sigma}_T^3\{-2q_1(T)\bar{K} + q_5(T)\bar{\Sigma}_T + 2\bar{\Sigma}_T^2\}] \\ & + \bar{K}(1 - \Phi(-\bar{K}/\sqrt{\bar{\Sigma}_T}))\Bigg\}, \end{aligned} \tag{3.6}$$

where $n(x;a,b)$ denotes the normal density function with mean a and variance b, $\Phi(x)$ is the cumulative distribution function of the standard normal distribution, and $q_1(t)$– $q_5(t)$ are given in Appendix A.

3.2. Barrier option pricing formula

Until now, we have discussed the third-order chaos expansion approximation and ignored the sum of integrated Itô stochastic integrals higher than fourth-order. However, it requires somewhat tedious and messy algebra, so we consider the second-order approximation for barrier option pricing.

In other words, we further approximate S_t and $f_X(x)$ as

$$S_t \approx F(0,t)(1 + a_1(t) + a_2(t)),$$

where $a_1(t) \approx f_0(t)$ and $a_2(t)$ is defined in Lemma 2.1, and

$$f_X(x) = n(x; 0, \Sigma_T)\left[\frac{q(T)}{(\sqrt{\Sigma_T})^3}\left\{\left(\frac{x}{\sqrt{\Sigma_T}}\right)^3 - 3\left(\frac{x}{\sqrt{\Sigma_T}}\right)\right\} + 1\right],$$

where $\Sigma_T \approx \int_0^T f_0^2(s)\mathrm{d}s$ and

$$q(T) \approx \int_0^T f_0^2(s)\left(\int_0^s f_0^2(u)\mathrm{d}u\right)\mathrm{d}s + \rho\int_0^T f^{(1)}(s)f_0(s)\left(\int_0^s \lambda_2(s,u)f_0(u)\mathrm{d}u\right)\mathrm{d}s.$$

This paper extends the approximation method developed by Funahashi and Higuchi (2017). For this purpose, let us consider a random variable

$$\tilde{S}(W_t) = F(0,t)\left[1 + \sqrt{\Sigma_t}h_1\left(\frac{W_t}{\sqrt{t}}\right) + \frac{q(t)}{\Sigma_t}h_2\left(\frac{W_t}{\sqrt{t}}\right)\right],$$

where $h_n(x)$ denotes the Hermite polynomial of order n defined by

$$h_n(x) = (-1)^n \mathrm{e}^{x^2/2}\frac{\mathrm{d}^n}{\mathrm{d}x^n}\mathrm{e}^{-x^2/2}, \quad n = 1, 2, \ldots,$$

with $h_0(x) = 1$.[4] Since $h_1(\frac{W_t}{\sqrt{t}}) = \frac{1}{\sqrt{t}}\int_0^t \mathrm{d}W_s$ and $h_2(\frac{W_t}{\sqrt{t}}) = \frac{2}{t}\int_0^t(\int_0^s \mathrm{d}W_u)\mathrm{d}W_s$, Theorem A.1 can be applied to obtain the distribution of $\tilde{X}_t := \tilde{S}_t/F(0,t) - 1$, denoted as $f_{\tilde{X}}$. An important observation at this point is that up to the second-order chaos expansion approximation, the distribution of S_t and $\tilde{S}(W_t)$ coincide exactly:

$$f_{X_t}(x) = f_{\tilde{X}_t}(x), \tag{3.7}$$

for all x and t.

Moreover, we can estimate pathwise difference

$$Y_t := \frac{S_t - \tilde{S}(W_t)}{F(0,t)} = b_1(t) + b_2(t),$$

where

$$\begin{aligned} b_1(t) &= \int_0^t \beta(s)\mathrm{d}W_s, \\ b_2(t) &= \int_0^t f_0(s)\left(\int_0^s f_0(u)\mathrm{d}W_u\right)\mathrm{d}W_s + \int_0^t f_0^{(1)}(s)\left(\int_0^s \lambda_2(s,u)\mathrm{d}\bar{W}_u\right)\mathrm{d}W_s \\ &\quad - \frac{2q(t)}{t\Sigma_t}\int_0^t\left(\int_0^s \mathrm{d}W_u\right)\mathrm{d}W_s, \end{aligned}$$

[4]For example, we have $h_1(x) = x$, $h_2(x) = x^2 - 1$, $h_3(x) = x^3 - 3x$, etc.

with $\beta(s) = f_0(s) - \sqrt{\Sigma_t/t}$. Note that Y_t has same structure as S_t in Lemma 2.1. Thus, we can compute the probability distribution function of Y_T. The proof of the following theorem is given in Appendix B.

Theorem 3.2. *The probability distribution function of Y_T is approximated as*

$$f_{Y_T}(x) \approx \begin{cases} \delta(x), & \Lambda_T = 0, \\ n(x; 0, \Lambda_T)\left[\dfrac{r(T)}{(\sqrt{\Lambda_T})^3}\left\{\left(\dfrac{x}{\sqrt{\Lambda_T}}\right)^3 - 3\left(\dfrac{x}{\sqrt{\Lambda_T}}\right)\right\} + 1\right], & \textit{otherwise}, \end{cases}$$

where $\delta(x)$ is the Dirac delta function, $\Lambda_t = \int_0^t \beta^2(s)\mathrm{d}s$, and

$$\begin{aligned} r(t) = &\int_0^t f_0(s)\beta(s)\left(\int_0^s f_0(u)\beta(u)\mathrm{d}u\right)\mathrm{d}s \\ &+\rho \int_0^t f_0^{(1)}(s)\beta(s)\left(\int_0^s \lambda_2(s,u)\beta(u)\mathrm{d}u\right)\mathrm{d}s \\ &-\frac{2q(t)}{t\Sigma_t}\int_0^t \beta(s)\left(\int_0^s \beta(u)\mathrm{d}u\right)\mathrm{d}s. \end{aligned}$$

Note that, if r, κ, and θ are zero, $f_0(t) = f(\sigma_0)$ becomes constant and, hence, $\Lambda_t = 0$ for all t. Thus, the following results are immediate consequences of Theorem 3.2:

Corollary 3.2. *If r, κ, and θ are zero, up to the second-order chaos expansion, the probability density function of Y_T is approximated as*

$$f_{Y_T}(x) \approx \delta(x).$$

Remark 3.1. As we shall show numerically in the following section, even in the case that r, κ, and θ are not zero, when Λ_t is small for $\forall t \in [0, T]$, these differences are negligible for barrier option pricing. Funahashi and Higuchi (2017) applied Doob's martingale inequality to show numerically that this mimicked process, $\tilde{S}(W_t)$, becomes a pathwise (or strong) approximation of the original one, S_t, except for negligible size of events.

By using these facts, our approximation in this paper is to approximate the barrier option (3.4) as

$$C^B(T, K) \approx \mathrm{e}^{-rT}\mathbb{E}[g(\tilde{S}(W_T))]. \tag{3.8}$$

Then, the barrier option price (3.8) can be computed as follows. The sketch of the proof is given in Appendix C.

Proposition 3.1. *Suppose that the assumptions in Appendix C are satisfied and $\Lambda_t \approx 0$ for $\forall t \in [0, T]$. Then, the value of an up-and-in barrier option with barrier* *level B, maturity T, and strike K is approximated as*

$$
\begin{aligned}
C^B(T,K) \approx\ & \frac{\mathrm{e}^{\Omega_T}\mathrm{e}^{-rT}}{2\sqrt{2\pi}\Sigma_T}\left(\mathrm{e}^{-\frac{(\omega^1_T(K)-\dot{\omega}_T)^2}{2T}}X_1(T) - \mathrm{e}^{-\frac{(\omega^1_T(B)-\dot{\omega}_T)^2}{2T}}X_2(T)\right) \\
& + \frac{\mathrm{e}^{\Omega_T}\mathrm{e}^{-tT}}{2\Sigma_T}X_3(T)\left(\Phi\left(\frac{\omega^1_T(B)-\dot{\omega}_T}{\sqrt{T}}\right) - \Phi\left(\frac{\omega^1_T(K)-\dot{\omega}_T}{\sqrt{T}}\right)\right) \\
& + \frac{S_0}{\sqrt{2\pi}\Sigma_T^{\frac{5}{2}}}\mathrm{e}^{-\frac{\bar{B}^2}{2\Sigma_T}}\{\bar{B}^2(\bar{B}+\bar{K})q(T) - \bar{K}q(T)\Sigma_T + \Sigma_T^{\frac{3}{2}}\} \\
& + S_0\bar{K}\left(1 - \Phi\left(\frac{\bar{B}}{\sqrt{\Sigma_T}}\right)\right), \qquad (3.9)
\end{aligned}
$$

where $\bar{K} := 1 - K/F(0,T)$, $\bar{B} = B/F(0,T) - 1$, *and* Φ *is the cumulative distribution function of the standard normal distribution. The explicit formulas of* Ω_T, $\omega^1_T(K)$, $\dot{\omega}_T$, *and* $X_1(T) - X_3(T)$ *are defined in Appendix C.*

4. Numerical Examples

This section is devoted to numerical experience to examine the accuracy of the approximation and test the effect of parameters on the derivative prices.

For this purpose, we calculate the approximated option prices given by Theorem 3.1 and Proposition 3.1, and compare them with Monte Carlo (MC) simulation results. The benchmark values for the Asian options are computed by MC with 500,000 trials and 250 time steps, while those for the barrier options are simulated by 500,000 trials with three time steps; 12 (monthly), 50 (weekly), and 250 (daily) time steps per year. In all the table and figures below, "WIC" denotes the option prices calculated by the approximation formula given in Sec. 3, and "MC" indicates the prices computed by the MC simulation.

Now, we specify the fractional volatility model used in this section. Originally, Comte and Renault (1998) introduced a model in which log-volatility follows fractional Brownian motion. Recently, it seems that there is a general consensus that estimated log-volatility from high frequency data behaves as a fractional Brownian motion (Bayer *et al.*, 2016). Following this tendency, we suppose that the volatility in (2.1) is given as

$$f(\sigma) = \nu \exp\{\sigma\},$$

where ν is constant.

First, we perform an accuracy check of our approximation formulas in Sec. 3. The parameters are set to $S_0 = 100$, $\sigma_0 = 0.3$, $r = 0.03$, $\nu = 0.15$, $\epsilon = 0.1$, $\rho = -0.5, 0.5$, $K = 90, 100, 110$ and $H = 0.1, 0.5, 0.9$. For the barrier options, we examine the long ($T = 1$) and short maturity ($T = 0.5$) cases with $B = 110$, while fixing $\theta = 0.09$ and $\kappa = 0.3$. For the Asian options, we test $\theta = 1$ and $\theta = 0.05$ cases, while fixing $T = 1$ and $\kappa = 2$. The results are listed in Tables 1 and 2 for the barrier option prices and the Asian option prices, respectively. It is observed that the difference between our approximation and the Monte Carlo result is reasonably small for practical use. However, the barrier option prices computed by MC always produce smaller values than our approximation results. Since prices are calculated for barrier options with continuous monitoring, it is necessary to pick a smaller time step. In addition, it is known that MC for fBMs is difficult to perform because of the non-Markovian nature (Kijima and Tam, 2013). Since the convergence speed is very slow and computational cost is expensive, the simulation is stopped after 500,000 trials with daily time steps. These facts suggest that this MC is not enough to generate accurate option prices in the fractional volatility model, although they are satisfactory for practical use.

The average MC simulation times for one barrier option are 1 min 43 s, 8 min 48 s, and 35 h 13 min for the monthly, weekly, and daily simulation, respectively, while our approximation takes only 0.472 sec. Of course, these approximation formulas are not always perfect. According to numerical tests, the error becomes gradually larger for the options with long maturity and high volatility. Particularly, when ν and γ are high and/or maturity is long, this approximation produces unsatisfactory results. If this is not accurate enough, higher order approximation may be needed, which can be derived easily, although tedious, by following the same discussions given in this paper. See Funahashi and Higuchi (2017) for details.

Next, we examine the impact of the fractional volatility to the barrier option.[5] In the following, we translate the present value of the option price to the corresponding barrier option's Black implied volatility, σ_b, to understand the price level intuitively. To be more specific, we consider the volatility σ_b, which satisfies

$$C^B(T,K) = -S_0\left(\frac{B}{S_0}\right)^{2\lambda} N(-y) + K\mathrm{e}^{-rT}\left(\frac{B}{S_0}\right)^{2\lambda-2} N(-y+\sigma\sqrt{T}), \tag{4.1}$$

where $\lambda = (r + \frac{1}{2}\sigma_b^2)/\sigma_b^2$ and $y = \ln(B/(S_0K))/(\sigma_b\sqrt{T}) + \lambda\sigma_b\sqrt{T}$. The formula in the right-hand side of the above equation is the pricing formula of the up-and-in barrier options under Black–Scholes setting. For more information, see, e.g., Chapter 24 of Hull (2009). The base parameters are set as $S_0 = 100$, $\sigma_0 = 0.5$, $r = 0$, $\kappa = 0.0001$, $\theta = \kappa\sigma_0$, $\rho = -0.5$, $\nu = 0.15$, and $B = 105$.

[5]The Asian option shows the same tendency so we only list the results of the barrier option in this paper.

Table 1. Barrier option prices calculated by our approximation formula in proposition 3.1 and those of MC results. "WIC" denotes the option prices calculated by the approximation formula, while "MC" indicates the prices computed by the Monte Carlo simulation with daily, weekly, and monthly time steps. The parameters are set to $S_0 = 100$, $\sigma_0 = 0.3$, $r = 0.03$, $\nu = 0.15$, $\epsilon = 0.1$, $\kappa = 0.3$, $\theta = 0.09$, $\rho = -0.5, 0.5$, $K = 90, 100, 110$, $T = 0.5, 1$, $B = 110$, and $H = 0.1, 0.5, 0.9$.

				MC (Daily)						MC (Weekly)						MC (Monthly)					
	WIC			0.1		0.5		0.9		0.1		0.5		0.9		0.1		0.5		0.9	
K/H	0.1	0.5	0.9		Diff		Diff		Diff		Diff		Diff		Diff		Diff		Diff		Diff
T = 0.5 $\rho = -0.5$																					
90	10.90	10.81	10.80	10.63	−0.27	10.58	−0.23	10.58	−0.22	10.31	−0.59	10.27	−0.54	10.26	−0.54	10.27	−0.63	10.24	−0.57	10.23	−0.56
100	6.20	6.16	6.16	6.13	−0.07	6.10	−0.06	6.10	−0.06	6.11	−0.09	6.08	−0.08	6.08	−0.07	6.40	0.20	6.38	0.23	6.38	0.23
110	2.59	2.63	2.66	2.64	0.04	2.64	0.00	2.66	0.00	2.72	0.13	2.73	0.09	2.74	0.09	3.11	0.52	3.12	0.49	3.13	0.48
T = 0.5 $\rho = 0.5$																					
90	10.88	10.74	10.75	10.62	−0.26	10.55	−0.19	10.55	−0.21	10.29	−0.59	10.24	−0.50	10.24	−0.51	10.25	−0.63	10.22	−0.51	10.22	−0.53
100	6.21	6.15	6.15	6.18	−0.03	6.12	−0.04	6.11	−0.05	6.15	−0.06	6.10	−0.05	6.09	−0.06	6.44	0.23	6.40	0.25	6.39	0.24
110	2.77	2.73	2.70	2.83	0.07	2.74	0.02	2.71	0.01	2.90	0.14	2.83	0.10	2.80	0.09	3.26	0.49	3.20	0.48	3.18	0.47
T = 1 $\rho = -0.5$																					
90	14.78	14.69	14.66	14.61	−0.17	14.54	−0.15	14.52	−0.14	14.44	−0.34	14.38	−0.32	14.36	−0.31	14.36	−0.42	14.31	−0.39	14.29	−0.38
100	9.47	9.42	9.42	9.45	−0.01	9.39	−0.03	9.38	−0.03	9.43	−0.03	9.38	−0.04	9.37	−0.04	9.64	0.17	9.60	0.17	9.59	0.17
110	5.33	5.35	5.37	5.39	0.06	5.35	0.00	5.36	0.00	5.43	0.10	5.40	0.05	5.41	0.04	5.72	0.39	5.70	0.35	5.71	0.34
T = 1 $\rho = 0.5$																					
90	14.53	14.48	14.51	14.47	−0.05	14.41	−0.07	14.42	−0.09	14.30	−0.23	14.25	−0.22	14.26	−0.25	14.24	−0.29	14.20	−0.27	14.21	−0.30
100	9.39	9.37	9.38	9.46	0.07	9.38	0.02	9.37	0.00	9.43	0.05	9.38	0.01	9.37	−0.01	9.64	0.25	9.59	0.23	9.58	0.21
110	5.48	5.46	5.45	5.60	0.11	5.50	0.04	5.47	0.02	5.62	0.14	5.54	0.08	5.51	0.06	5.89	0.41	5.83	0.37	5.80	0.35

Table 2. Asian option prices calculated by our approximation formula in Theorem 3.1 and those of MC results. "WIC" denotes the option prices calculated by the approximation formula, while "MC" indicates the prices computed by the Monte Carlo simulation. "Diff" shows the difference between "WIC" and "MC". The parameters are set to $S_0 = 100$, $\sigma_0 = 0.3$, $r = 0.03$, $\nu = 0.15$, $\epsilon = 0.1$, $\kappa = 2$, $\rho = -0.5, 0.5$, $K = 90, 100, 110$, $\theta = 1, 0.05$, $T = 1$, and $H = 0.1, 0.5, 0.9$.

	WIC			MC			Diff		
K/H	0.1	0.5	0.9	0.1	0.5	0.9	0.1	0.5	0.9
$\theta = 1$ $\rho = -0.5$									
90	12.27	12.23	12.21	12.24	12.20	12.18	0.03	0.03	0.03
100	5.72	5.68	5.68	5.69	5.65	5.65	0.03	0.03	0.03
110	2.06	2.06	2.07	2.04	2.03	2.05	0.02	0.02	0.02
$\theta = 1$ $\rho = 0.5$									
90	12.17	12.17	12.18	12.14	12.14	12.15	0.03	0.03	0.03
100	5.72	5.68	5.68	5.68	5.65	5.64	0.03	0.03	0.03
110	2.18	2.13	2.11	2.17	2.11	2.09	0.02	0.02	0.02
$\theta = 0.05$ $\rho = -0.5$									
90	11.86	11.82	11.81	11.84	11.81	11.79	0.02	0.02	0.02
100	4.97	4.94	4.94	4.96	4.93	4.93	0.01	0.01	0.01
110	1.43	1.43	1.44	1.42	1.42	1.43	0.00	0.00	0.00
$\theta = 0.05$ $\rho = 0.5$									
90	11.77	11.77	11.78	11.75	11.76	11.77	0.02	0.02	0.02
100	4.97	4.94	4.94	4.95	4.92	4.92	0.01	0.01	0.01
110	1.54	1.49	1.47	1.54	1.49	1.47	0.00	0.00	0.00

Figure 1 reports the barrier option's Black implied volatility surface for the three cases; $H = 0.1$ (upper-panel), $H = 0.5$ (middle-panel), and $H = 0.9$ (lower-panel). When $H = 0.1$, the shape of the volatility surface increases faster with respect to maturity than the standard stochastic volatility model (middle-panel). On the other hand, when $H = 0.9$ the shape of the volatility surface increases slower than the standard stochastic volatility model ($H = 0.5$). This phenomenon can be explained by the long-memory feature of the fractional volatility, as expected by Comte and Renault (1998) and examined numerically by Funahashi and Kijima (2017a) for European option case. The maximum and minimum difference of the volatility level between $H = 0.1$ and $H = 0.9$ are 1.25% and −1.00%, respectively. This is larger than the market bid-ask spread and, hence, cannot be neglected.

Figure 2 indicates the barrier option's Black implied volatility surface, for four cases; $\kappa = 0.0001$ and $T = 0.1$ (upper-left), $\kappa = 4$ and $T = 0.1$ (upper-right), $\kappa = 0.0001$ and $T = 1$ (lower-right), and $\kappa = 4$ and $T = 1$ (lower-right). For all cases, we set $\theta = \sigma_0\kappa$. From the upper-left and upper-right panel show that the

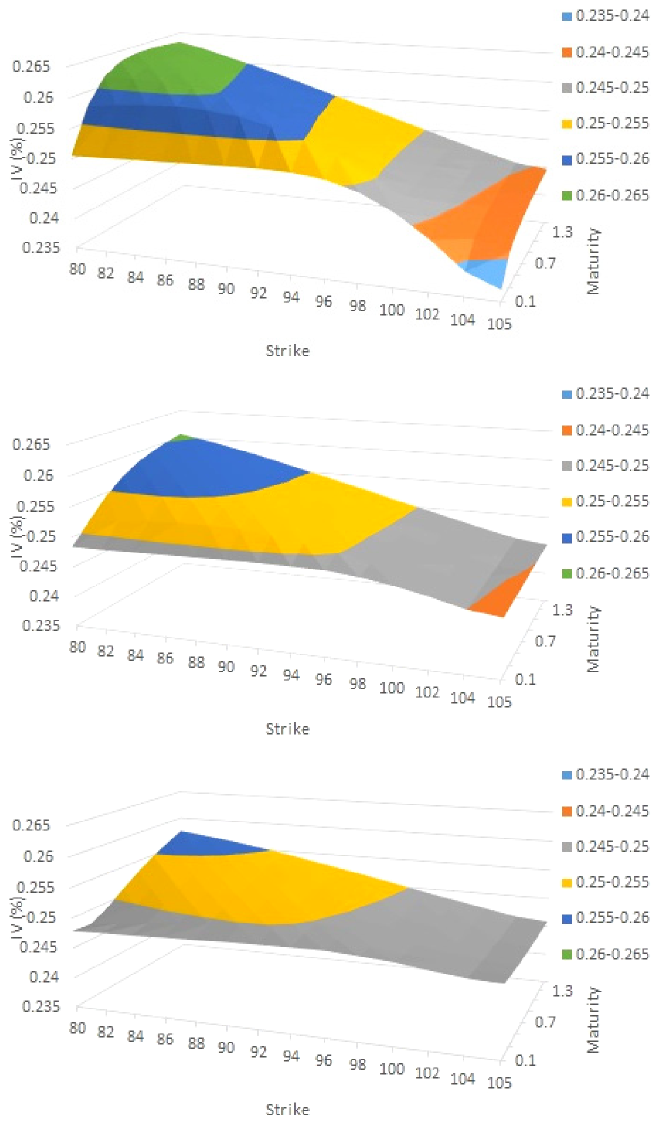

Fig. 1. Up-and-in barrier option's Black implied volatility $\sigma_b(K,T)$ (defined in (4.1) and labeled "IV") for the three cases; $H = 0.1$ (upper-panel), $H = 0.5$ (middle-panel), and $H = 0.9$ (lower-panel). Other parameters are set as $S_0 = 100$, $\sigma_0 = 0.5$, $r = 0$, $\kappa = 0.0001$, $\theta = \kappa\sigma_0$, $\rho = -0.5$, $\nu = 0.15$, and $B = 105$.

shapes of volatility surface are close in the short maturity case. However, if the speed of mean reversion is fast, the implied volatility slope with respect to H becomes milder and almost flat as the maturity lengthen. On the other hand, when the speed of mean reversion is slow, the implied volatility slope with respect to H

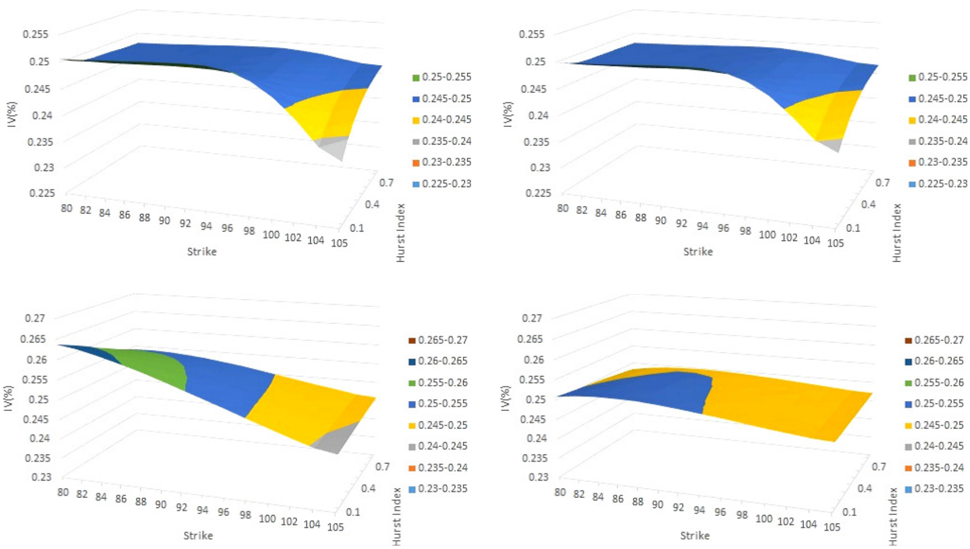

Fig. 2. Up-and-in barrier option's Black implied volatility $\sigma_b(K,H)$ (defined in (4.1) and labeled "IV") for the four cases; $\kappa = 0.0001$ and $T = 0.1$ (upper left-hand side), $\kappa = 4$ and $T = 0.1$ (upper right-hand side), $\kappa = 0.0001$ and $T = 1$ (lower left-hand side), and $\kappa = 4$ and $T = 1$ (lower right-hand side). For all cases, we set $\theta = v_0\kappa$. Other parameters are set as $S_0 = 100$, $\sigma_0 = 0.5$, $r = 0$, $\rho = -0.5$, $\nu = 0.15$, and $B = 105$.

remains even in the long maturity. Thus, the impact of the Hurst index remains when the speed of mean reversion is slow even in the long maturity case. Paradoxically, if the speed of mean reversion is fast, the impact of Hurst index reduces as the maturity lengthen.

Finally, we check the impact of the Hurst index on the distribution of the Asian Price, $f_{A_t}(x)$, defined in (3.5). Figure 3 shows the $f_{A_t}(x)$ with three cases; $H = 0.1$, $H = 0.5$, and $H = 0.9$. The upper two panels describe $\kappa = 1 \times 10^{-15}$ and the lower two panels indicate $\kappa = 1$. Other parameters are set as $\theta = \sigma_0\kappa$, $S_0 = 100$, $\sigma_0 = 0.3$, $\epsilon = 0.15$, $\rho = 0.8$, and $\nu = 0.15$. On the other hand, the left-hand side panels show short maturity case ($T = 0.25$) and right-hand side panels show long maturity case ($T = 1$). From the figures, the distribution of $H = 0.1$ and $H = 0.9$ approach to that of $H = 0.5$ in long maturity cases. Moreover, it can be observed that when the speed of mean reversion is fast, the convergence speed is fast, while when the speed of mean reversion is slow, the convergence speed is slow. This result is consistent with the results in Fig. 2.

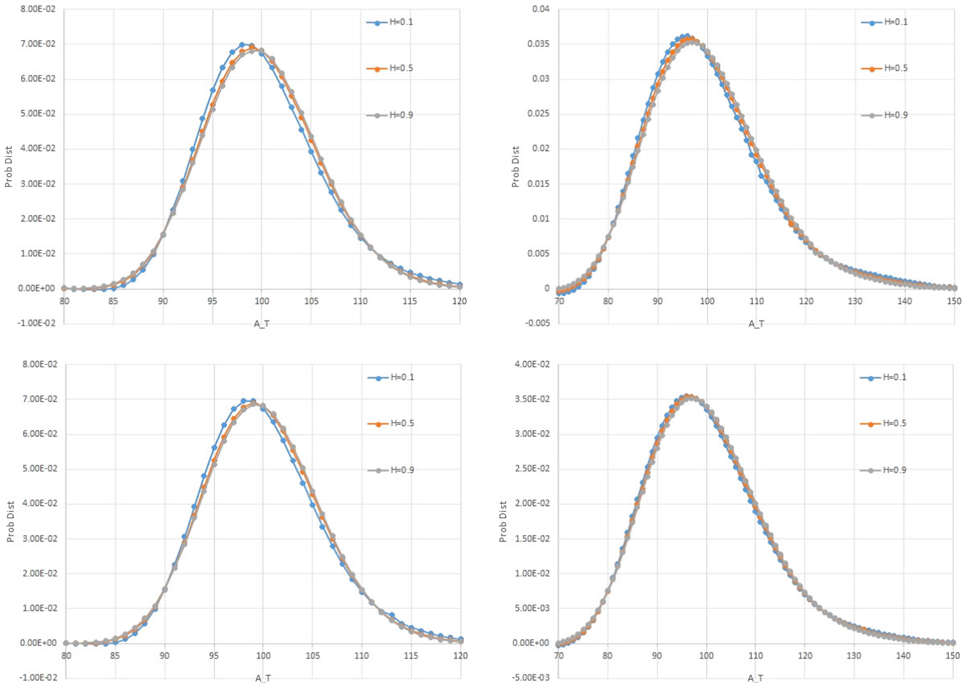

Fig. 3. The distribution of the Asian Price, $f_{A_t}(x)$ with three cases; $H = 0.1$, $H = 0.5$, and $H = 0.9$. The upper two panels describe $\kappa = 1 \times 10^{-15}$ and lower two panels indicates $\kappa = 1$. On the other hand, the left-hand side panels show short maturity case ($T = 0.25$) and right-hand side panels show long maturity case ($T = 1$). Other parameters are set as $\theta = \sigma_0 \kappa$, $S_0 = 100$, $\sigma_0 = 0.3$, $\epsilon = 0.15$, $\rho = 0.8$, and $\nu = 0.15$.

5. Conclusion

This paper proposes approximation formulas for the Asian and barrier options when the underlying asset process follows a fractional volatility model. Option prices using the proposed approximation are compared by MC simulations. Through the comparison tests, we conclude that they are accurate enough for practical purposes.

It is known that MC for fBMs is difficult to perform because of the non-Markovian nature; the convergence speed is very slow and computational cost is expensive. On contrary, our approximation formula requires at most three dimensional integrals and is therefore fast to compute.

Using the proposed formulas, we examined the impact of the Hurst index H on the path-dependent options. Through numerical experience, it is observed that, when $H < 0.5$, the shape of the volatility surface increases faster with respect to maturity than $H = 0.5$, while, when $H > 0.5$, the shape of the volatility surface increases slower than $H = 0.5$. This phenomenon can be explained by the long-memory feature of the fractional volatility.

Overall, our finding is that if the speed of mean reversion is fast, the impact of H on option prices diminish as the maturity lengthens. On the other hand, if the speed of mean reversion is slow, the impact of H remains even in the long maturity case.

These results may bring an important message for practitioners who use the standard Brownian motions for option pricing.

Appendix A. Proof of Theorem 3.1

Since, S_t is approximated by a truncated sum of Wiener-Itô stochastic integrals in Corollary 3.1, we can apply the following theorem and an approximation of the density function can be obtained. The proof can be found in Funahashi and Kijima (2014).

Theorem A.1. *The probability density function of X_T is approximated as*

$$\begin{aligned} f_{X_T}(x) = n(x;0,\bar{\Sigma}_T) &- \frac{\partial}{\partial x}\{\mathbb{E}[\bar{a}_2(T)|\bar{a}_1(T)=x]n(x;0,\bar{\Sigma}_T)\} \\ &- \frac{\partial}{\partial x}\{\mathbb{E}[\bar{a}_3(T)|\bar{a}_1(T)=x]n(x;0,\bar{\Sigma}_T)\} \\ &+ \frac{1}{2}\frac{\partial^2}{\partial x^2}\{\mathbb{E}[\bar{a}_2(T)^2|\bar{a}_1(T)=x]n(x;0,\bar{\Sigma}_T)\} + \cdots. \end{aligned} \tag{A.1}$$

Further, the conditional expectations can be evaluated explicitly, by just following the standard arguments. From (D.1), (D.2) and (D.3) in Appendix D, respectively, we obtain

$$\mathbb{E}[\bar{a}_2(T)|\bar{a}_1(T)=x] = q_1(T)\left(\frac{x^2}{\bar{\Sigma}_T^2} - \frac{1}{\bar{\Sigma}_T}\right),$$

$$\mathbb{E}[\bar{a}_3(T)|\bar{a}_1(T)=x] = q_2(T)\left(\frac{x^3}{\bar{\Sigma}_T^3} - \frac{3x}{\bar{\Sigma}_T^2}\right),$$

$$\mathbb{E}[\bar{a}_2^2(T)|\bar{a}_1(T)=x] = q_3(T)\left(\frac{x^4}{\bar{\Sigma}_T^4} - \frac{6x^2}{\bar{\Sigma}_T^3} + \frac{3}{\bar{\Sigma}_T^2}\right) + q_4(T)\left(\frac{x^2}{\bar{\Sigma}_T^2} - \frac{1}{\bar{\Sigma}_T}\right) + q_5(T),$$

where

$$\begin{aligned} q_1(T) = &\int_0^T \bar{f}_0(T,s)\bar{\gamma}(T,s)\left(\int_0^s f_0(u)\bar{\gamma}(T,u)\mathrm{d}u\right)\mathrm{d}s \\ &+ \rho\int_0^T \bar{f}^{(1)}(T,s)\bar{\gamma}(T,s)\left(\int_0^s \lambda_2(s,u)\bar{\gamma}(T,u)\mathrm{d}u\right)\mathrm{d}s, \end{aligned}$$

$$
\begin{aligned}
q_2(T) = {} & \int_0^T \bar{f}_0(T,s)\bar{\gamma}(T,s)\left(\int_0^s f_0(u)\bar{\gamma}(T,u)\left(\int_0^u f_0(r)\bar{\gamma}(T,r)\mathrm{d}r\right)\mathrm{d}u\right)\mathrm{d}s \\
& + \rho\int_0^T \bar{f}_0(T,s)\bar{\gamma}(T,s)\left(\int_0^s f_0^{(1)}(u)\bar{\gamma}(T,u)\left(\int_0^u \lambda_2(u,r)\bar{\gamma}(T,r)\mathrm{d}r\right)\mathrm{d}u\right)\mathrm{d}s \\
& + \rho\int_0^T \bar{f}_0^{(1)}(T,s)\bar{\gamma}(T,s)\left(\int_0^s f_0(u)\bar{\gamma}(T,u)\left(\int_0^u \lambda_2(s,r)\bar{\gamma}(T,r)\mathrm{d}r\right)\mathrm{d}u\right)\mathrm{d}s \\
& + \rho\int_0^T \bar{f}_0^{(1)}(T,s)\bar{\gamma}(T,s)\left(\int_0^s \lambda_2(s,u)\bar{\gamma}(T,u)\left(\int_0^u f_0(r)\bar{\gamma}(T,r)\mathrm{d}r\right)\mathrm{d}u\right)\mathrm{d}s \\
& + \rho^2\int_0^T \bar{f}_0^{(2)}(T,s)\bar{\gamma}(T,s) \\
& \times\left(\int_0^s \lambda_2(s,u)\bar{\gamma}(T,u)\left(\int_0^u \lambda_2(s,r)\bar{\gamma}(T,r)\mathrm{d}r\right)\mathrm{d}u\right)\mathrm{d}s, \\
q_3(T) = {} & q_1^2(T), \\
q_4(T) = {} & \sum_{i=1}^3 q_{4,i}(T), \\
q_5(T) = {} & \int_0^T \bar{f}_0(T,s)^2\left(\int_0^s f_0(u)^2\mathrm{d}u\right)\mathrm{d}s + \int_0^T (\bar{f}_0^{(1)}(T,s))^2\left(\int_0^s \lambda_2^2(s,u)\mathrm{d}u\right)\mathrm{d}s \\
& + 2\rho\int_0^T \bar{f}_0(T,s)\bar{f}_0^{(1)}(T,s)\left(\int_0^s \lambda_2(s,u)f_0(u)\mathrm{d}u\right)\mathrm{d}s,
\end{aligned}
$$

where

$$
\begin{aligned}
q_{4,1}(T) = {} & 2\int_0^T \bar{f}_0(T,s)\bar{\gamma}(T,s)\left(\int_0^s \bar{f}_0(T,u)\bar{\gamma}(T,u)\left(\int_0^u f_0(r)^2\mathrm{d}r\right)\mathrm{d}u\right)\mathrm{d}s \\
& + 2\int_0^T \bar{f}_0(T,s)\bar{\gamma}(T,s)\left(\int_0^s \bar{f}_0(T,u)f_0(u)\left(\int_0^u f_0(r)\bar{\gamma}(T,r)\mathrm{d}r\right)\mathrm{d}u\right)\mathrm{d}s \\
& + \int_0^T \bar{f}_0(T,s)^2\left(\int_0^s f_0(u)\bar{\gamma}(T,u)\mathrm{d}u\right)^2\mathrm{d}s, \\
q_{4,2}(t) = {} & 2\int_0^T \bar{f}_0^{(1)}(T,s)\bar{\gamma}(T,s) \\
& \times\left(\int_0^s \bar{f}_0^{(1)}(T,u)\bar{\gamma}(T,u)\left(\int_0^u \lambda_2(s,r)\lambda_2(u,r)\mathrm{d}r\right)\mathrm{d}u\right)\mathrm{d}s \\
& + 2\rho^2\int_0^T \bar{f}_0^{(1)}(T,s)\bar{\gamma}(T,s)
\end{aligned}
$$

$$\times\left(\int_0^s \bar{f}_0^{(1)}(T,u)\lambda_2(s,u)\left(\int_0^u \lambda_2(u,r)\bar{\gamma}(T,r)\mathrm{d}r\right)\mathrm{d}u\right)\mathrm{d}s$$
$$+\rho^2\int_0^T (\bar{f}_0^{(1)}(T,s))^2\left(\int_0^s \lambda_2(s,u)\bar{\gamma}(T,u)\mathrm{d}u\right)^2\mathrm{d}s,$$

$$q_{4,3}(T) = 2\rho\int_0^T \bar{f}_0(T,s)\bar{\gamma}(T,s)$$
$$\times\left(\int_0^s \bar{f}_0^{(1)}(T,u)\bar{\gamma}(T,u)\left(\int_0^u \lambda_2(u,r)f_0(r)\mathrm{d}r\right)\mathrm{d}u\right)\mathrm{d}s$$
$$+2\rho\int_0^T \bar{f}_0^{(1)}(T,s)\bar{\gamma}(T,s)$$
$$\times\left(\int_0^s \bar{f}_0(T,u)\bar{\gamma}(T,u)\left(\int_0^u \lambda_2(s,r)f_0(r)\mathrm{d}r\right)\mathrm{d}u\right)\mathrm{d}s$$
$$+2\rho\int_0^T \bar{f}_0(T,s)\bar{\gamma}(T,s)$$
$$\times\left(\int_0^s f_0(u)\bar{f}_0^{(1)}(T,u)\left(\int_0^u \lambda_2(u,r)\bar{\gamma}(T,r)\mathrm{d}r\right)\mathrm{d}u\right)\mathrm{d}s$$
$$+2\rho\int_0^T \bar{f}_0^{(1)}(T,s)\bar{\gamma}(T,s)$$
$$\times\left(\int_0^s \bar{f}_0(T,u)\lambda_2(s,u)\left(\int_0^u f_0(r)\bar{\gamma}(T,r)\mathrm{d}r\right)\mathrm{d}u\right)\mathrm{d}s$$
$$+2\rho\int_0^T \bar{f}_0(T,s)\bar{f}_0^{(1)}(T,s)$$
$$\times\left(\int_0^s f_0(u)\bar{\gamma}(T,u)\mathrm{d}u\right)\left(\int_0^s \lambda(s,u)\bar{\gamma}(T,u)\mathrm{d}u\right)\mathrm{d}s.$$

By substitute the conditional expectations into (A.1), the approximated density function, denoted by $\tilde{f}_{X_T}(x)$, can be expressed as

$$\tilde{f}_{X_T}(x) = \frac{1}{2}n(x;0,\bar{\Sigma}_T)\left[\frac{q_3(T)}{\bar{\Sigma}_T^3}h_6\left(\frac{x}{\sqrt{\bar{\Sigma}_T}}\right)+\frac{(2q_2(T)+q_4(T))}{\bar{\Sigma}_T^2}h_4\left(\frac{x}{\sqrt{\bar{\Sigma}_T}}\right)\right.$$
$$\left.+\frac{2q_1(T)}{\left(\sqrt{\bar{\Sigma}_T}\right)^3}h_3\left(\frac{x}{\sqrt{\bar{\Sigma}_T}}\right)+\frac{q_5(T)}{\bar{\Sigma}_T}h_2\left(\frac{x}{\sqrt{\bar{\Sigma}_T}}\right)+2\right], \tag{A.2}$$

where $h_n(x)$ denotes the Hermite polynomial defined in Sec. 3.

Appendix B. Proof of Theorem 3.2

In order to calculate the probability distribution of Y_t, we first derive an approximated characteristic function of Y_t and then invert back to derive an approximation of the probability distribution of Y_t.

Let the characteristic function of Y_t be $\Psi(\xi) = \mathbb{E}[\mathrm{e}^{i\xi Y_t}]$. We approximate it as

$$\begin{aligned}\Psi(\xi) &\approx \mathbb{E}[\mathrm{e}^{\{i\xi(b_1(t)+b_2(t))\}}] \\ &= \mathbb{E}[\mathrm{e}^{i\xi b_1(t)}(1 + i\xi b_2(t) + R_3)],\end{aligned}$$

where R_3 consists of the third or higher-order multiple stochastic integrals.

But, since

$$\begin{aligned}|\mathbb{E}[\mathrm{e}^{i\xi b_1(t)} R_3]| &\leq \mathbb{E}[|\mathrm{e}^{i\xi b_1(t)} R_3|] \\ &\leq (\mathbb{E}[|\mathrm{e}^{i\xi b_1(t)}|^2])^{\frac{1}{2}} (\mathbb{E}[|R_3|^2])^{\frac{1}{2}} \\ &= (\mathbb{E}[|R_3|^2])^{\frac{1}{2}} \approx 0,\end{aligned}$$

we regard $\mathbb{E}[\mathrm{e}^{i\xi b_1(t)} R_3] \approx 0$ as for the previous case.[6]

Note that, when $\Lambda_t = 0$, $b_1(t) = 0$ for all $t \in [0, T]$. Taking the conditional expectation on $b_1(t)$, we then have

$$\Psi(\xi) \approx \begin{cases} 1, & \beta(t) = 0 \quad \text{for } \forall t \in [0, T], \\ \mathbb{E}[\mathrm{e}^{i\xi b_1(t)}] + i\xi \mathbb{E}[\mathrm{e}^{i\xi b_1(t)} \mathbb{E}[b_2(t) \mid b_1(t)]], & \text{otherwise}. \end{cases}.$$

The conditional expectations can be evaluated explicitly, by using the formulas in Appendix D. Namely, we obtain

$$\mathbb{E}[b_2(t) | b_1(t) = x] = r(t)\left(\frac{x^2}{\Lambda_t^2} - \frac{1}{\Lambda_t}\right), \tag{B.1}$$

where $r(t)$ is defined in Theorem 3.2.

Since $b_1(t)$ follows a normal distribution with zero mean and variance Λ_t, we can apply the following inversion formula. The proof can be found in Funahashi and Kijima (2015).

Lemma B.1. *Suppose that X follows a normal distribution with zero mean and variance Σ. Then, for any polynomial functions $f(x)$ and $g(x)$, we have*

$$\frac{1}{2\pi} \int_{\mathcal{R}} \mathrm{e}^{-iky} g(-ik) \mathbb{E}[f(X)\mathrm{e}^{ikX}]\mathrm{d}k = g\left(\frac{\partial}{\partial y}\right) f(y) n(y; 0, \Sigma),$$

where $n(x; a, b)$ denotes the normal density function with mean a and variance b.

Finally, by applying Lemma B.1 to each term of the characteristic function, we obtain the desired result.

[6] See Funahashi and Kijima (2015) for details.

Appendix C. Proof of Proposition 3.1

Let us define the first moment that the mimicked asset price, $\tilde{S}(W_t)$, hits the barrier by

$$\tilde{\tau} := \inf\{t \geq 0 : \tilde{S}(W_t) \leq B\}. \tag{C.1}$$

Since $\tilde{S}(W_t)$ is a quadratic function of the Brownian motion W_t, the quadratic formula is applicable.

The determinant is denoted by

$$D_t(B) := \Sigma_t^3 + 4\left(\frac{B}{F(0,t)} - 1\right)q(t)\Sigma_t + 4q^2(t),$$

and the solutions of the equation with respect to W_t are indicated by

$$\omega_t^{1,2}(B) := -\frac{\sqrt{t}(\Sigma_t^{\frac{3}{2}} \mp \sqrt{D_t(B)})}{2q(t)}.$$

Then, we can translate the problem of solving first hit probability of asset process into the problem of solving that of the Wiener process:

$$\tilde{\tau}_i := \inf\{t \geq 0 : W_t = \omega_t^i(B)\},$$

for $i = 1, 2$. In the following, we only consider the case $D_t(B) \geq 0$ with $P(\tilde{\tau}_1 < \tilde{\tau}_2) \approx 1$. The verification of this assumption is provided in Sec. 5.1 of Funahashi and Higuchi (2017).

Thus, the passage time, τ, in (3.3) of the underlying asset price to the barrier can be approximated as

$$\tau \approx \tilde{\tau}_1. \tag{C.2}$$

Next, to simplify the problem let us consider a random variable

$$Z_t := W_t - \omega_t^1(B) + \omega_0^1(B),$$

with its running maximum

$$M_t^Z := \max_{0 \leq s \leq t} Z_s.$$

Note that, since

$$\inf\{t \geq 0 : W_t = \omega_t^1(B)\} = \inf\{t \geq 0 : Z_t = \omega_0^1(B)\},$$

we have

$$\tau \approx \inf\{t \geq 0 : Z_t = \omega_0^1(B)\}.$$

We then use Girzanov's theorem to translate the results on the Brownian motions W_t under $\mathbb{Q}$ to the results on the Brownian motion Z_t under $\mathbb{P}$. More precisely, we suppose that $\omega_t^1(B)$ is differentiable on t and the derivative, $\alpha(t) := -\frac{\partial}{\partial t}\omega_t^1(B)$, satisfies the Lipschitz condition and put

$$\xi(W_t) := \exp\left(-\int_0^t \alpha(s)\mathrm{d}W_s - \frac{1}{2}\int_0^t \alpha^2(s)\mathrm{d}s\right), \quad t \le T,$$

and define a probability measure $\mathbb{P}$ by

$$P(A) := \mathbb{E}[\chi_A \cdot \xi(W_t)] \quad \text{for } \forall A \in \mathcal{F}_t, \tag{C.3}$$

then Z_t is a standard Brownian motion with respect to the probability law $\mathbb{P}$ for $t \le T$. In the following, we denote $\mathbb{E}^{\mathbb{P}}[\,\cdot\,]$ by the expectation with respect to probability measure $\mathbb{P}$.

For future references, we approximate $1/\xi(W_T)$ by a polynomial function of W_T:

$$\begin{aligned} 1/\xi(W_t) = {} & \exp\left(\int_0^t \alpha^2(s)\mathrm{d}s\right)\exp\left(\int_0^t \alpha(s)\mathrm{d}W_s - \frac{1}{2}\int_0^t \alpha^2(s)\mathrm{d}s\right) \\ & \approx \mathrm{e}^{\Omega_T}\left[1 + \phi\sqrt{\Omega_T}h_1\left(\frac{W_t}{\sqrt{t}}\right) + \frac{1}{2}\Omega_T h_2\left(\frac{W_t}{\sqrt{t}}\right)\right], \end{aligned} \tag{C.4}$$

where $\phi := \int_0^T \alpha(s)\mathrm{d}s / |\int_0^T \alpha(s)\mathrm{d}s|$ and $\Omega_T = \int_0^t \alpha^2(s)\mathrm{d}s$. The accuracy of this approximation is studied numerically in Funahashi and Higuchi (2017).

Now, we are ready to derive an approximation formula for European up-and-in barrier options with strike K and maturity T written on the asset S_t.

Suppose that $B > K$[7], we have

$$\begin{aligned} C^B(T,K) &\approx \mathrm{e}^{-\int_0^T r(s)\mathrm{d}s}\mathbb{E}\big[\tilde{S}(W_T) - K; \tilde{S}(W_T) > K, \tilde{\tau} < T\big] \\ &= \mathrm{e}^{-\int_0^T r(s)\mathrm{d}s}\mathbb{E}\big[\tilde{S}(W_T) - K; \tilde{S}(W_T) \in (K,B), \tilde{\tau} < T\big] \\ &\quad + \mathrm{e}^{-\int_0^T r(s)\mathrm{d}s}\mathbb{E}\big[\tilde{S}(W_T) - K; B < \tilde{S}(W_t)\big]. \end{aligned} \tag{C.5}$$

Further, from (C.3), we can say that

$$\begin{aligned} &\mathbb{E}\big[\tilde{S}(W_T) - K; \tilde{S}(W_T) \in (K,B), \tilde{\tau} < T\big] \\ &\quad \approx \mathbb{E}\big[\tilde{S}(W_T) - K; W_T \in (\omega_T^1(K), \omega_T^1(B)), \tilde{\tau} < T\big] \\ &\quad = \mathbb{E}^{\mathbb{P}}\big[(\tilde{S}(Z_T + \hat{\omega}_T) - K)/\xi(Z_T + \hat{\omega}_T); Z_T \in (\bar{\omega}_T, \omega_0^1(B)), M_T^Z > \omega_0^1(B)\big], \end{aligned}$$

where $\hat{\omega}_T = \omega_T^1(B) - \omega_0^1(B)$ and $\bar{\omega}_T = \omega_T^1(K) - \hat{\omega}_T$.

[7] Since, when $B \le K$ the up-and-in barrier option reduces to the ordinary call option and the price is given by the Black–Scholes formula, we concentrate in the case $B > K$.

But since Z_t is a standard Brownian motion under $\mathbb{P}$, the probability distribution function is known as

$$P(Z_t \in a, M_t^Z \geq b) = \frac{1}{\sqrt{2\pi t}} \mathrm{e}^{-\frac{(2b-a)2}{2t}}.$$

(See e.g., Karazas and Shreve (1998) for proof.)

Thus, from the definition of $\tilde{S}$ and (C.4), the first term in the last equation of (C.5) can be computed as

$$\begin{aligned}
&\mathbb{E}^{\mathbb{P}}\left[(\tilde{S}(Z_T+\hat{\omega}_T)-K)/\xi(Z_T+\hat{\omega}_T); Z_T \in (\bar{\omega}_T, \omega_0^1(B)), M_T^Z > \omega_0^1(B)\right] \\
&= \frac{1}{\sqrt{2\pi T}} \int_{\bar{\omega}_T}^{\omega_0^1(B)} (\tilde{S}(z+\hat{\omega}_T)-K)/\xi(z+\hat{\omega}_T) \mathrm{e}^{-\frac{(z-2\omega_0^1(B))2}{2T}} \mathrm{d}z \\
&\approx \frac{\mathrm{e}^{\Omega_T}}{2\sqrt{2\pi}\Sigma_T}\left(\mathrm{e}^{-\frac{(\omega_T^1(K)-\dot{\omega}_T)2}{2T}} X_1(T) - \mathrm{e}^{-\frac{(\omega_T^1(B)-\dot{\omega}_T)2}{2T}} X_2(T)\right) \\
&\quad + \frac{\mathrm{e}^{\Omega_T}}{2\Sigma_T} X_3(T)\left(\Phi\left(\frac{\omega_T^1(B)-\dot{\omega}_T}{\sqrt{T}}\right) - \Phi\left(\frac{\omega_T^1(K)-\dot{\omega}_T}{\sqrt{T}}\right)\right)
\end{aligned}$$

where Φ is the cumulative distribution function of the standard normal distribution, $\dot{\omega}_T = \omega_T^1(B) + \omega_0^1(B)$, and $X_i(T)$ being defined as

$$\begin{aligned}
X_1(T) := {} & F(0,T)q(T)(\omega_T^1(K)+\dot{\omega}_T)[(\omega_T^1(K))^2 + (\dot{\omega}_T)^2]\Omega_T T^{-\frac{3}{2}} \\
& + F(0,T)[(\omega_T^1(K))^2 + \omega_T^1(K)\dot{\omega}_T + (\dot{\omega}_T)^2](2\phi q(T)\sqrt{\Omega_T} + \Sigma_T^{\frac{3}{2}}\Omega_T)T^{-1} \\
& + (\omega_T^1(K)+\dot{\omega}_T)\Sigma_T[F(0,T)(2\phi\sqrt{\Sigma_T\Omega_T} + \Omega_T) - K\Omega_T]T^{-\frac{1}{2}} \\
& + F(0,T)q(T)[\omega_T^1(K)(2+\Omega_T) + \dot{\omega}_T(2+3\Omega_T)]T^{-\frac{1}{2}} \\
& + F(0,T)\Sigma_T[2\phi\sqrt{\Omega_T} + \sqrt{\Sigma_T}(2+\Omega_T)] \\
& + 2\phi(F(0,T)q(T) - K\Sigma_T)\sqrt{\Omega_T},
\end{aligned}$$

$$\begin{aligned}
X_2(T) := {} & F(0,T)q(T)(\omega_T^1(B)+\dot{\omega}_T)[(\omega_T^1(B))^2 + (\dot{\omega}_T)^2]\Omega_T T^{-\frac{3}{2}} \\
& + F(0,T)[(\omega_T^1(B))^2 + \omega_T^1(B)\dot{\omega}_T + (\dot{\omega}_T)^2](2\phi q(T)\sqrt{\Omega_T} + \Sigma_T^{\frac{3}{2}}\Omega_T)T^{-1} \\
& + (\omega_T^1(B)+\dot{\omega}_T)\Sigma_T[F(0,T)(2\phi\sqrt{\Sigma_T\Omega_T} + \Omega_T) - K\Omega_T]T^{-\frac{1}{2}} \\
& + F(0,T)q(T)[\omega_T^1(B)(2+\Omega_T) + \dot{\omega}_T(2+3\Omega_T)]T^{-\frac{1}{2}} \\
& + F(0,T)\Sigma_T[2\phi\sqrt{\Omega_T} + \sqrt{\Sigma_T}(2+\Omega_T)] \\
& + 2\phi(F(0,T)q(T) - K\Sigma_T)\sqrt{\Omega_T},
\end{aligned}$$

and

$$
\begin{aligned}
X_3(T) := {} & F(0,T)q(T)\dot{\omega}_T^4\Omega_T T^{-2} + F(0,T)\dot{\omega}_T^3(2\phi q(T)\sqrt{\Omega_T} + \Sigma_T^{\frac{3}{2}}\Omega_T)T^{-\frac{3}{2}} \\
& + \dot{\omega}_T^2\Big\{2\phi F(0,T)\Sigma_T\sqrt{\Sigma_T\Omega_T} + F(0,T)\Sigma_T\Omega_T + 2F(0,T)q(T)(1+2\Omega_T) \\
& - K\Sigma_T\Omega_T\}T^{-1} + 2F(0,T)\dot{\omega}_T(2\phi q(T)\sqrt{\Omega_T} + \Sigma_T^{\frac{3}{2}}(1+\Omega_T) \\
& + \phi\Sigma_T\sqrt{\Omega_T})T^{-\frac{1}{2}} - 2\phi K\dot{\omega}_T\sqrt{\Omega_T}\Sigma_T T^{-\frac{1}{2}} \\
& + 2F(0,T)\Sigma_T(1+\phi\sqrt{\Sigma_T\Omega_T}) + 2F(0,T)q(T)\Omega_T - 2K\Sigma_T.
\end{aligned}
$$

Here we used the fact that $\omega_T^1(B) > \omega_T^1(K)$.

Furthermore, since the distribution of $\tilde{X}_T$ has already at the hand in (3.7), the second term in Eq. (C.5) can be evaluated as

$$
\begin{aligned}
& \mathbb{E}[\tilde{S}(W_T) - K; B < \tilde{S}(W_T)] \\
& \quad = F(0,T)\int_{\bar{B}}^{\infty}(x+\bar{K})f_{\tilde{X}}(x)\mathrm{d}x \\
& \quad = \frac{F(0,T)}{\sqrt{2\pi}\Sigma_T^{\frac{5}{2}}}\mathrm{e}^{-\frac{\bar{B}^2}{2\Sigma_T}}\{\bar{B}^2(\bar{B}+\bar{K})q(T) - \bar{K}q(T)\Sigma_T + \Sigma_T^3\} + F(0,T) \\
& \qquad \times \bar{K}\left(1 - \Phi\left(\frac{\bar{B}}{\sqrt{\Sigma_T}}\right)\right),
\end{aligned}
$$

where $\bar{K} := 1 - K/F(0,T)$ and $\bar{B} = B/F(0,T) - 1$.

Finally, these results are combined to obtain the desired result.

Appendix D. Conditional Expectation

The formulas have been already given in our paper Funahashi and Kijima (2014) but for the reader's convenience we give them again.

Let W_t^i, $i = 1,\ldots,5$, be standard Brownian motions with correlation $\mathrm{d} < W_t^i, W_t^j >= \rho_{i,j}\mathrm{d}t$, and let $y_i(x)$, $i = 1,\ldots,5$ be deterministic functions of time. Moreover, let $\Sigma := \int_0^T y_1^2(t)\mathrm{d}t$, and denote $J_T(y_1) = \int_0^T y_1(t)\mathrm{d}W_t^1$.

Then, the following formulas are known:

$$
E\left[\int_0^T y_3(t)\left(\int_0^t y_2(s)\mathrm{d}W_s^2\right)\mathrm{d}W_t^3 | J_T(y_1) = x\right] = v_1\left(\frac{x^2}{\Sigma^2} - \frac{1}{\Sigma}\right), \tag{D.1}
$$

where

$$
v_1 = \int_0^T \rho_{1,3}y_3(t)y_1(t)\left(\int_0^t \rho_{1,2}y_2(s)y_1(s)\mathrm{d}s\right)\mathrm{d}t. \tag{D.2}
$$

$$E\left[\int_0^T y_4(t)\left(\int_0^t y_3(s)\left(\int_0^s y_2(u)\mathrm{d}W_u^2\right)\mathrm{d}W_s^3\right)\mathrm{d}W_t^4 | J_T(y_1)=x\right]$$
$$= v_2\left(\frac{x^3}{\Sigma^3}-\frac{3x}{\Sigma^2}\right),$$

where

$$v_2 = \int_0^T \rho_{1,4}y_4(t)y_1(t)\left(\int_0^t \rho_{1,3}y_3(s)y_1(s)\left(\int_0^s \rho_{1,2}y_2(u)y_1(u)\mathrm{d}u\right)\mathrm{d}s\right)\mathrm{d}t.$$

$$\begin{aligned}E\Bigg[&\left(\int_0^T y_3(t)\left(\int_0^t y_2(s)\mathrm{d}W_s^2\right)\mathrm{d}W_t^3\right)\\ &\times\left(\int_0^T y_5(t)\left(\int_0^t y_4(s)\mathrm{d}W_s^2\right)\mathrm{d}W_t^3\right)|J_T(y_1)=x\Bigg]\\ &= v_3\left(\frac{x^4}{\Sigma^4}-\frac{6x^2}{\Sigma^3}-\frac{3}{\Sigma^2}\right)+v_4\left(\frac{x^2}{\Sigma^2}-\frac{1}{\Sigma}\right)+v_5,\end{aligned} \tag{D.3}$$

where

$$\begin{aligned}v_3 = &\left(\int_0^T \rho_{1,3}y_3(t)y_1(t)\left(\int_0^t \rho_{1,2}y_2(t)y_1(t)\mathrm{d}s\right)\mathrm{d}t\right)\\ &\times\left(\int_0^T \rho_{1,5}y_5(t)y_1(t)\left(\int_0^t \rho_{1,4}y_4(t)y_1(t)\mathrm{d}s\right)\mathrm{d}t\right),\end{aligned}$$

$$\begin{aligned}v_4 = &\int_0^T \rho_{1,3}y_3(t)y_1(t)\left(\int_0^t \rho_{1,5}y_5(s)y_1(s)\left(\int_0^s \rho_{2,4}y_4(u)y_2(u)\mathrm{d}u\right)\mathrm{d}s\right)\mathrm{d}t\\ &+\int_0^T \rho_{1,5}y_5(t)y_1(t)\left(\int_0^t \rho_{1,3}y_1(s)y_3(s)\left(\int_0^s \rho_{2,4}y_4(u)y_2(u)\mathrm{d}u\right)\mathrm{d}s\right)\mathrm{d}t\\ &+\int_0^T \rho_{1,3}y_3(t)y_1(t)\left(\int_0^t \rho_{2,5}y_2(s)y_5(s)\left(\int_0^s \rho_{1,4}y_4(u)y_1(u)\mathrm{d}u\right)\mathrm{d}s\right)\mathrm{d}t\\ &+\int_0^T \rho_{1,5}y_5(t)y_1(t)\left(\int_0^t \rho_{3,4}y_3(s)y_4(s)\left(\int_0^s \rho_{1,2}y_2(u)y_1(u)\mathrm{d}u\right)\mathrm{d}s\right)\mathrm{d}t\\ &+\left\{\int_0^T \rho_{3,5}y_5(t)y_3(t)\left(\int_0^t \rho_{1,2}y_2(s)y_1(s)\mathrm{d}s\right)\left(\int_0^t \rho_{1,4}y_4(s)y_1(s)\mathrm{d}s\right)\mathrm{d}t\right\},\end{aligned}$$

$$v_5 = \int_0^T \rho_{3,5}y_5(t)y_3(t)\left(\int_0^t \rho_{2,4}y_4(u)y_2(u)\mathrm{d}u\right)\mathrm{d}t.$$

References

Alòs, E, JA León and J Vives (2007). On the short-time behavior of the implied volatility for jump-diffusion models with stochastic volatility, *Finance and Stochastics*, 11, 571–589.

Bayer, C, P Friz and J Gatheral (2016). Pricing under rough volatility, *Quantitative Finance*, 16, 887–904.

Bollerslev, T (1986). Generalized autoregressive conditional heteroskedasticity, *Journal of Econometrics*, 31, 307–327.

Bollerslev, T and HO Mikkelsen (1996). Fractionally integrated generalized autoregressive conditional heteroskedasticity, *Journal of International Economics*, 74, 3–30.

Cheridito, P (2003). Arbitrage in fractional Brownian motion models, *Finance and Stochastics*, 7, 533–553.

Comte, F and E Renault (1998). Long memory in continuous-time stochastic volatility model, *Mathematical Finance*, 8, 291–323.

Engle, FE and JP Andrew (2001). What good is a volatility model? *Quantitative Finance*, 1, 237–245.

Fukasawa, M (2011). Asymptotic analysis for stochastic volatility: Martingale expansion, *Finance and Stochastics*, 15, 635–654.

Funahashi, H and K Kijima (2015). A chaos expansion approach for the pricing of contingent claims, *Journal of Computational Finance*, 18, 27–58.

Funahashi, H and T Higuchi (2017). An analytical approximation for single barrier options under Stochastic Volatility Models, working paper.

Funahashi, H and M Kijima (2014). An Extension of the chaos expansion approximation for the pricing of exotic basket options, *Applied Mathematical Finance*, 21, 109–139.

Funahashi, H and M Kijima (2017a). Does the Hurst index matter for option prices under fractional volatility? *Annals of Finance*, 13(1), 55–74.

Funahashi, H and M Kijima (2017b). A Unified Approach for the Pricing of Options Relating to Averages, *Review of Derivatives Research*, forthcoming.

Gatheral, J, T Jaisson and M Rosenbaum (2014). Volatility is rough, Working Paper.

Guasoni, P (2006). No arbitrage with transaction costs, with fractional Brownian motion and beyond, *Mathematical Finance*, 16, 569–582.

Heston, SL (1993), A closed-form solution for options with stochastic volatility with applications to bond and currency options, *Review of Financial Studies*, 6, 327–343.

Hu, Y and B Øksendal (2003). Fractional white noise calculus and applications in finance, *Quantum Probability and Related Topics*, 6, 1–32.

Hull, J (2009), *Options, Futures, and Other Derivatives*, 7th Edn. Prentice Hall: USA.

Hull, J and A White (1987). The pricing of options on assets with stochastic volatilities, *Journal of Finance*, 42, 281–300.

Karazas, I and S Shreve (1998). *Brownian Motion and Stochastic Calculus*, Springer-Verlag: New York.

Kijima, M and CM Tam (2013). Fractional Brownian motions in financial models and their Monte Carlo simulation, *Theory and Applications of Monte Carlo Simulations*, March, 53–85.

Mandelbort, BB and JWV Ness (1968). Fractional Brownian motions, fractional noises and applications, *SIAM Review*, 10, 422–437.

Nelson, DB (1991). Conditional heteroskcdasticity in asset returns: A new approach, *Econometrica*, 59, 347–370.

Rogers, LCG (1997). Arbitrage with fractional Brownian motion, *Mathematical Finance*, 7, 95–105.

Schöbel, R and J Zhu (1999). Stochastic volatility with Ornstein–Uhlenbeck process: An extension, *European Finance Review*, 4, 23–46.

Sottinen, T (2001). Fractional Brownian motion, random walks and binary market models, *Finance and Stochastics*, 5, 343–355.

Xiao, WL, WG Zhang and YL Wang (2010). Pricing currency options in a fractional Brownian Motion with Jump, *Economic Modeling*, 27, 935–942.